Experimental and numerical analysis of the spray application on apple fruit in a bin for postharvest treatments

A. Ambaw[a, e, *], D. Dekeyser[b], T. Vanwalleghem[c], W. Van Hemelrijck[c], D. Nuyttens[b], M.A. Delele[a], H. Ramon[a], B. Nicolai[a, d], D. Bylemans[c], U. L. Opara [e,f] , P. Verboven[a]

[a] Division MeBioS – Postharvest Group, KU Leuven – University of Leuven, Willem de Croylaan 42, B-3001 Leuven, Belgium

[b] ILVO - Technology and Food Science Unit - Agricultural Engineering, B-9820 Merelbeke, Belgium,

[c] Research Station for Fruit Growing (pcfruit vzw), Mycology Department, B-3800 Sint-Truiden, Belgium,

[d] Flanders Centre of Postharvest Technology, Willem de Croylaan 42, B-3001 Leuven, Belgium

[e] Postharvest Technology Research Laboratory, South African Research Chair in Postharvest Technology, Department of Horticultural Science, Stellenbosch University , Stellenbosch 7602, South Africa

[f] Postharvest Technology Research Laboratory, South African Research Chair in Postharvest Technology, Department of Food Science, Stellenbosch University, Stellenbosch 7602, South Africa

*Corresponding author; email: tsige@sun.ac.za

Abstract

Postharvest treatment of fruit inside a cool room is gaining more interest to replace spray applications in the orchard. The efficacy of the application depends on the quality of the spray liquid and its distribution inside fruit bin. This work investigated the effect of different modes and settings of airflow delivery on the deposition amount and uniformity of the cold fogging spray deposition in a single bin. Room air circulation by means of evaporator fans was compared to an air suction configuration using a tunnel and suction fan. Deposition tests were conducted using a mineral chelate tracer solution and filter paper collectors placed on fruit. A computational fluid dynamics (CFD) model of the spraying process was developed to simulate

the airflow, droplet particle tracks and spray deposits on fruits. The model predicted well the position of maximum and minimum deposit and the relative differences between the different modes and settings of airflow delivery. Generally, deposition distributions were strongly non-uniform. Spray deposits on fruit using only room air circulation were very low. Using suction airflow that directs the spray through the bin improved spray deposition and uniformity. The effects of spraying under different suction pressures (50, 167, 314 and 500 Pa) across the bin using different droplet diameters (15, 100, 200 and 300 μm) was evaluated. Depending on the size, different effects were observed. Coarse droplets perform best in terms of uniformity of deposition with more lateral dispersion, whereas fine droplets have a very limited lateral dispersion, travels deep to the stack following the high-velocity air (better axial dispersion). By implementing multiple nozzles the poor lateral dispersion of fine droplets can be improved, hence, the desirable characteristics of fine droplets in penetrating into the stack (axial distribution) can be retained.

Keywords. Postharvest, fruit disease, biological control organism, spraying, computational fluid dynamics, simulation

1 Introduction

Postharvest spoilage of fruits and vegetables causes substantial economic loss (Barth et al. 2009.; Gustavsson et al., 2011). Much of this is due to micro-organisms causing rotting which is generally controlled by applying cooling and fungicides. Application of postharvest disease controlling substances inside the controlled environment of the cool room might be suitable. This method has been gaining attention and has replacing treatments in the orchard. Orchard spraying could lead to suboptimal results due to uncertain climate conditions and has been associated with environmental and health risks (Dekeyser et al., 2015, Duga et al., 2015, Mahajan et al., 2014). In addition, concerns on the use of fungicides in the fresh produce

industry have grown due to the development of pathogen resistance to many key fungicides, the lack of replacement fungicides, the negative public perception regarding the safety of pesticides and the consequent restrictions on fungicide use (Janisiewicz and Korsten, 2002).

There has been a strong interest in the development of alternative postharvest treatment techniques. One such alternative is the use of Biological Control Organisms (BCOs) which has emerged as an effective strategy to combat the incidence of postharvest decay of fruits and has been extensively investigated (Droby et al., 2003; Francesco and Mari, 2014). BCOs are organisms used to decrease inoculum or the disease-producing activity of a pathogen (Baker, 1987). Particularly, the use of BCOs together with low doses of fungicides appear more effective (Francesco and Mari, 2014).

Treatment after harvest is normally done during transport from the field to the storage room by bulk dipping, shower or spraying of harvested fruit. These treatment methods have several disadvantages: they increase the time between harvest and storage, physical damage and injury may occur on fruit during the treatment, and they could lead to cross contamination of pathogenic fungi. Interest to perform postharvest applications inside cold storage room has risen. Cold storage rooms are convenient to strictly control parameters such as temperature and humidity to suit the needs of the active agent (Wisniewski et al., 2001, 2007; Droby and Lechter, 2004). Spray applications on stacked fruit bins in cold storage room has been suggested (Dekeyser et al., 2015). In such application, penetration of the spray into the internal region of stack is crucial for the efficiency and uniformity of the application process. The amount and uniformity of deposition of the droplets should be known for proper dose calculation. This requires accurate characterization and understanding of the spraying process in the cool store environment and the affecting factors. It is already known that air circulation in the cool store room, fruit bin stacking, droplet diameter and velocity, and the position and orientation of the sprayer have an effect on the trajectory of sprayed droplets and their ultimate deposition on

solid surfaces in the cool store room (Delele et al., 2012a, 2012b, Nuyttens et al., 2007a, 2007b). Droplet diameter is a function of spraying equipment, the liquid formulation and the airflow, which has not been quantified to date for spray application techniques for BCOs in cool stores.

Due to the complexity of the problem, experimental methods alone may not be sufficient to fully understand the problem. Computational fluid dynamics (CFD) simulates the flow field generated by a spraying device and the subsequent trajectory and deposition of sprayed droplets in various applications. For pre-harvest applications, a CFD model of orchard spraying was used to study the effect of machinery setup, i.e. sprayed volume, use of fans, tractor speed, etc. to help compare different sprayers and their performance (Delele et al., 2007; Duga et al., 2015; Endalew et al., 2010). Delele et al., (2012a & 2012b) used CFD to assess the spray application by thermonebulisation of fungicide in a cold storage room and examined the effects of air circulation rate, circulation interval, stacking pattern, room design and bin design on fungicide particles flow and distribution. As such, CFD provides more detailed information of the actual process to support and explain the experimental observations. Furthermore, after validation of the CFD model, simulations can be performed to analyze different configurations and search for more optimal treatments.

The objective of the present work was to determine the suitability of spray applications of apple fruit in bins supported by airflow. A CFD model of the spraying process on a single bin was developed and validated experimentally. Then the validated model was applied to study the effects of airflow and droplet size on the spraying process efficiency and uniformity. Room air circulation by means of evaporator fans was compared to an air suction configuration using a tunnel and suction fan.

2 Materials and methods

2.1 Apple fruit and bin

A standard plastic bin for harvesting and storing apple fruit was used in this analysis. The bin has an external length, width and height of 1.20 m × 1.20 m × 0.74 m and had perforated side walls and bottom. The vent area proportion of the sides of the bin used in this study was 35 %. The bin contained 380 ± 20 kg randomly packed ‘Jonagold’ apple fruit.

2.2 Spray device

A Fontan® Starlet ULV 92 cold fogger with a 6 L spraying tank (Swingtec GmbH, Isny, Germany) was used for the experiment. The machine is electrically driven by a 1.5 kW motor. A turbine produces a high velocity air stream, which is further accelerated in the swirl vane of the nozzle system. This air stream causes suction in the solution pipe, and conveys the spray solution, which is atomized into droplets at the spray diffuser of the spray pistol. Prior to the tests, measurements were performed to determine the flow rate, droplet diameter spectrum, droplet velocity and the shape of the spray cone using a Phase Doppler Particle Analyzer (PDPA, Aerometrics Sunnyvale, CA, USA) at 0.50 m from the outlet opening (Nuyttens et al., 2007a). The liquid flow rate was estimated from the time taken to drain a 50% full spray tank.

2.3 Experiments

Two different test setups were used: spraying on a bin placed in a tunnel with suction configuration and spraying on a bin placed in a cold store room. The main difference between the two setups is that in the first case all the circulating air is drawn through the bin, while in the second case, the air mainly circulates around the bins.

For the suction tests; a filled standard bin (Fig. 1(a)) was wrapped with plastic foil. At one side of the bin, a box fitted with a centrifugal fan (Fig. 1(b), (c)) was used to generate a

suction pressure behind the stacked fruit (Fig. 1(d)). The spray device was placed 1.6 m away from the bin, 0.52 m from the floor and directed at the bin middle (0.6 m from either side of the bin) (Fig. 1(e)). The positioning of the spray device was visually set in such a way that the spray cone was fully formed before reaching the fruit stack. The suction effect of the fan draws the air and the sprayed droplets through the stacked fruit. The experiment was undertaken at two suction pressures of 314 and 167 Pa.

The second test setup was spraying in a cold storage room. This was accomplished by placing a single bin in a storage room with dimensions: 4.8 m (depth) × 4.2 m (width) × 4.0 m (height). The bin was not wrapped in plastic and there was no additional suction (0 Pa). Spraying was performed through an access window through the door of the cool store. The spray nozzle was 1.6 m away from the bin and 0.52 m from the floor and directed at the middle of the bin (0.6 m from one side of the stack). The air circulation fan of the cool store room was turned off during the spray application.

For each case, a solution of 1L of water with a mineral chelate tracer was sprayed during a period of 12 ± 1 min. Depositions were measured after completion of spraying and droplet settling. To sample droplet depositions, filter papers (with an average dimension of 29.2 cm × 2.5 cm) were wrapped around apple fruits placed at specified positions in the bin. A multiple mineral tracer methodology (Foqué et al., 2014) comprising of six different minerals was used to differentially quantify the droplet depositions. Tracer concentration was 10 g of each mineral chelate per liter of spray solution for all of the tracers used. The sampling and measuring procedure is discussed below.

2.4 Measurements

The airflow velocity generated by the spraying machine and the suction fan in the region between the stack and the sprayer was measured to obtain data for model validation of the air

jet approaching the stack. Measurements were at grid points on vertical planes 0.4 m apart as shown in Fig. 2 using an ultrasonic anemometer (WindMaster 3d, Gill Instruments, Lymington, Hampshire). Each point velocity measurement was recorded over a period of two minutes at a sampling frequency of 1s. Suction pressure was measured using a U-tube manometer and the corresponding air velocity leaving the suction fan was measured at sampling grid points at the exit of the fan to obtain the superficial air velocity through the bin.

To measure spray depositions, three experimental conditions were considered in two repetitions: two different suction pressures (314 and 167 Pa) and one with no suction by placing a bin in the cool room (0 Pa). Using the tracer technique, spray depositions corresponding to each test run were measured by calculating the amount of respective tracer minerals found on the sampled apples which were placed in a net-bag at 9 selected positions inside the stack as shown in Fig. 3 (a), (b) and (c). Droplet depositions were collected on filter papers wrapped around the equatorial region of five apple fruits per sampling position (Fig. 3 (d)).

2.5 Model formulation

2.5.1 Governing equations

A spray is a two-phase flow which consists of one disperse phase (droplets) and one continuous phase (air). The prediction of the flow of the continuous air phase was obtained by solving the single phase Reynolds Averaged Navier Stokes (RANS) equations with the shear stress transport (SST) k-ω turbulence model. This turbulence model combines the best of two worlds. The use of a k-ω formulation in the inner parts of the boundary layer makes the model directly usable all the way down to the wall through the viscous sub-layer. The SST formulation also switches to a k-ε behaviour in the free-stream and thereby avoids the common k-ω problem that the model is too sensitive to the free-stream turbulence properties (Menter, 1993). This

model has been discussed and validated extensively in previous studies for flow and cooling of spherical fruits (Defraeye et al., 2013b; 2012; Delele et al., 2007).

The dispersed phase was modeled by the Lagrangian particle tracking (LPT) method where a reasonable number of computational droplets representing a number of real droplets with the same properties, were traced through the flow field. The study used the experimentally measured size distribution of droplets generated by the Swingtech ULV device and the measured flow rate at the injection locating. The trajectory of each droplet particle was calculated by solving the displacement ($\boldsymbol{x}_d$) using forward Euler integration of the particle velocity over time step, δt .

$$\boldsymbol{x}_d^{\,n} = \boldsymbol{x}_d^{\,o} + \mathbf{u}_d^{\,o}\delta t \tag{3}$$

where the superscripts o and n refer to the old and new values respectively and $\mathbf{u}_d^{\,o}$ is the initial droplet velocity. The droplet velocity at the beginning of the time step is assumed to prevail over the entire step. At the end of each time step, the new droplet velocity is calculated from Eqn. (4), taking into account turbulent dispersion of the droplets.

$$m_d \frac{\partial(\mathbf{u}_d)}{\partial t} = \frac{1}{8}\pi\rho d^2 c_d \left|\mathbf{u}-\mathbf{u}_d\right|\left(\mathbf{u}-\mathbf{u}_d\right) + \frac{1}{6}\pi d^3\left(\rho_d-\rho\right)g \tag{4}$$

where m_d is the droplet mass (kg), d is the droplet diameter (m), $\mathbf{u}$ is the continuous fluid velocity (m s^{-1}), $\mathbf{u}_d$ is the discrete droplet velocity (m s^{-1}), c_d is the drag coefficient, ρ_d is the discrete droplet density (kg m^{-3}), ρ is the density of the continuous phase (kg m^{-3}), g is the gravitational acceleration (m s^{-2}). The right side of Eqn. (4) contains the forces acting on the droplet which affect the droplet acceleration. In our approach, forces with negligible influence over the droplet acceleration or fate were neglected and only the drag and buoyancy forces were considered.

The drag coefficient (c_d) was calculated using an empirical correlation developed by Haider and Levenspiel (Haider & Levenspiel, 1989):

$$c_d = \frac{24}{\mathrm{Re}}(1 + 0.186 R_e^{0.653}) + \frac{0.437 R_e}{7135 + R_e} \quad (6)$$

where Re is the particle Reynolds number, defined by:

$$R_e = \frac{\rho |\mathbf{u} - \mathbf{u}_d| d}{\mu} \quad (7)$$

Upon hitting a surface, the fate of droplets is not well understood since they may stick, break up, or rebound. The droplet-wall interaction is a complex phenomenon involving the droplet impact energy and Weber number (Dahneke, 1971; Jain, 2015; Delele et al., 2016). However, to reduce the computation time, this study assumed that the surfaces trap the droplet when the droplet contacts the surface, and presumably covers also the cases where the droplet is captured at a close by position after bouncing or splitting. As this study considers average deposition in discrete zones of the bins and not punctual profiles, this approach should be sufficient.

2.5.2 The model geometry and boundary conditions

The model accounted geometric details of the stacked spheres, the void space between them and the bin. The position, size and shape of the vent-holes of the bin were accurately reproduced. Fruits were assumed dumped in a random manner into the bin. The discrete element (DE) modeling technique was used to simulate the dumping of 2000 spheres having a diameter that randomly varied between 80 mm and 85 mm into the bin. The DE method is a numerical technique for solving Newton's equation of motion of an assembly of interacting spheres. The gravitational force, collisions between spheres and collisions between spheres and walls were accounted in the DE method (Tijskens et al., 2003). Then, the coordinate location and size of each sphere from the DE model was used to generate the stack geometry for the CFD model. The value of the void fraction in the bin was 0.43.

Two different model geometries and boundary conditions were used to model the suction and the cool room setups. The model for the suction experiments is presented in Fig. 4 (a) and the model for the spraying in a room in Fig. 4 (b). Geometric and flow symmetry were assumed which justified reducing the models to half of the setups. The model geometries include the nozzle position, 1.6 m away, pointing directly horizontal and spraying on the stack. The spray nozzle was represented by an 8 mm cylinder located at the symmetry plane. The boundary conditions at the circular outlet of the nozzle were specified according to the measured airflow rate, spraying rate, droplet velocity, droplet size distribution and the spray plume characteristics. The result of the spray characterization is given in section 3.1. 500,000 sample poly-sized droplets, assumed spherical in shape, were released at 21 m s^{-1} from the cylinder outlet at a spraying rate of the device. The droplet size distribution of the injected spray was obtained experimentally and implemented at the boundary (Fig. 5).

For the model corresponding to the suction experiment, the inlet to the computational domain was represented as an opening boundary with pressure equal to atmospheric. The top and side faces of the region in front of the stack were open to the atmosphere and hence defined by an opening boundary condition with pressure equal to atmospheric. The bottom (floor) of the whole assembly was a no slip boundary. Surfaces of the fruit, the plastic sheet, the bin, the suction box and the fan were no slip boundaries. A circular cross section representing the fan outlet was set to an opening boundary condition with the measured suction pressure applied.

For the model corresponding to spraying in a cool store room (0 Pa), the walls, ceiling, floor, door, surfaces of the cooling unit, surfaces of the fruit bin and surfaces of the fruits were considered as no slip boundaries. For the purpose of assessing the effect of air circulation on the spray distribution inside the room, the air circulation fan was included in the CFD model. To do this, the region occupied by the cooling unit was isolated as a separate fluid domain bounded by solid walls (top, bottom and sides of the cooling unit). The inlet and outlet of the

cooling unit were interfaced with the cool store room. To model the air driving effect of the axial fan, a momentum source was added in the domain representing the cooling unit. The magnitude of the momentum source was gauged to give the required air circulation rate in the cool store room. Hence, the CFD model realistically reproduced the air circulation inside the cool store room (air and droplets drawn into the cooling unit from the cool store room, passes through it and expelled back to the room).

2.5.3 Solution procedures

The model equations were solved with the finite volume method. The domains were discretized using tetrahedral mesh elements. Mesh dependency was analyzed based on the difference in values of droplet depositions. A mesh dependence study was made using the grid convergence index (GCI) based on the Richardson extrapolation (Roache, 1994). For the GCI to be valid, three grids that give three solutions in asymptotic range were used. The mesh sensitivity test was performed first using 100000 sample droplets. Then, the optimization of the sensitivity of the model with respect to the number of sample droplets was conducted on the optimum mesh density. To do this, grid sizes of 2×10^6, 4×10^6 and 8×10^6 elements were used. In the simulation, the trajectories of all sample droplets from the point of injection to point of interaction with domain boundaries were calculated. The model enforces all particles that hit a wall to become part of the wall film, regardless of their impact velocity or impact angle. This way, wall depositions were calculated at every computational node on solid surfaces in the domain. From this, area average deposition values ($\mu L\ cm^{-2}$) at 3 sub-parts in the bin (dividing the fruit stack into 3 blocks) of the three grid setups were computed and compared. Based on this procedure, the fine and coarse grids have an average discretization error of 0.2% and 3.4%, respectively. Taking the simulation time into consideration, the actual simulations were undertaken using 6×10^6 elements. A similar procedure for the model corresponding to the spraying in a room gives a number of mesh elements equal to approximately 6.5×10^6.

The sensitivity of the simulation with respect to the total number of sample droplets to be tracked was also assessed by varying the number of droplets released from 100,000 to 1,000,000. The predicted droplet depositions remained constant above 500,000 droplets for the tunnel model as well as the model of the spraying in a room. Hence, in this study the total number of sample particles released from the nozzle in all the simulations was 500,000. A single full simulation took 72 and 120 h for the tunnel and room spraying models on a 64-bit, Intel $^{(R)}$ Core $^{(TM)}$ 2 Quad CPU, 3 GHz, 8 Gb RAM, Windows 7 PC.

3 Results and discussion

3.1 Spray characteristics

The Fontan® Starlet ULV 92 cold fogger produces a full, cone-shaped, plume with a round impact area at a spraying rate of 5.2 L h^{-1}. The fogger generates an air flow rate of 32 m^3 h^{-1}. The plume has a cone angle of 35°. The diameter and velocity distribution of the droplets are shown in Fig. 5 (a) and (b), respectively. The median volumetric droplet diameter and droplet velocity are about 30 µm and 5.8 m s^{-1}, respectively.

3.2 Validation of the CFD model

Fig. 6 shows the results of the measured and simulated air velocities in the suction experiment. Each point velocity measurement shown in Fig. 6 was average of values recorded over a period of two minutes at a sampling frequency of 1s. Due to turbulent velocity fluctuations the standard deviations on the experimental air velocities were large. Air leaves the nozzle as a high-velocity jet (≈ 21 m s^{-1}), not shown in Fig. 6, and decreases quickly to 3.2 and 3.7 m s^{-1} peak velocity at 40 cm from the nozzle outlet for the 167 and 314 Pa suction pressures (Fig. 6 (a) and (d)), respectively. The airflow profile was apparently an axi-symmetric jet close

290 to the nozzle (Fig.6 (a) and (d)) and laterally disperses with distance from the nozzle (Fig. 6 (c)
291 and (f)). Near the stack the suction effect gets prominent and airflow velocity increases in
292 magnitude. Also, the airflow velocity increases with distance from the floor. The suction fan
293 draws air from the surroundings into the bin while sprayer jet decays. The superficial air
294 velocity through the bin was 0.71 and 0.85 m s^{-1} at suction pressures of 167 and 314 Pa,
295 respectively, as calculated from the measured airflow velocity at fan exit and the bin cross-
296 sectional area perpendicular to the airflow direction. The model accurately predicted the
297 velocity profiles with a root mean square error (RMSE) of 0.15 m s^{-1}. The high and low airflow
298 regions were accurately captured by the CFD model. For the room treatment, the validation of
299 the model with respect to air flow inside the same cool store room was previously reported
300 (Delele et al., 2012a).

301 Fig. 7 summarizes the measured and simulated spray depositions. Generally, deposition
302 was low in the central region of the bin and high at the peripheries in all the cases. In the suction
303 tunnel, positions (1), (4) and (9), being close to the inlet region, had relatively high depositions.
304 In these regions depositions were generally above 10 µL cm^{-2} and could reach up to 40 µL cm^{-2}
305 , position (4) being the highest deposition region. On the other hand, positions (2), (3), (5), (6),
306 (7) and (8) were regions with very low depositions. Here depositions were below 0.5 µL cm^{-2}.
307 There was no significant difference (t-test shows $p = 0.26$) between the 167 and 314 Pa suction
308 pressures. However, the result of the room spraying was clearly distinct: it had very low overall
309 deposition. The maximum measured deposition was only 1.64 µL cm^{-2}. In this situation droplets
310 bypassed the bin and deposited on non-target surfaces (floor, walls, ceiling, and bin surfaces).

311 The high and low deposition regions were accurately identified by the CFD model and
312 droplet deposition was predicted with an average R^2 value of 0.90 and 0.70 for the tunnel and
313 the room spraying, respectively. Hence, the stick-to-wall assumption is sufficiently realistic in

314 that it predicted the depositions with good accuracy. Accuracy of the model of the room
315 spraying was lower due to its relatively higher computational complexity.

316 3.3 Effect of air velocity on the droplet distribution

317 In this section, we use the CFD model to analyze the effects of changing airflow settings in the
318 different regimes. For the suction regime, two more extreme suction pressures (50 and 500 Pa)
319 than in the experiment were used. For the room air circulation regime, fans operating at a mean
320 outlet velocity of 2 m s^{-1} and 4 m s^{-1} were added for comparison. All simulations were based
321 on initial and boundary conditions as obtained for the Fontan® spray device.

322 3.3.1 Airflow profile inside the fruit bin

323 Fig. 8 compares the magnitude of the air velocity in the stack internals using velocity
324 stream lines on the symmetry plane bisecting the bin for one of the suction and room air
325 circulation cases, respectively. A clear difference between the two airflow patterns can be
326 observed. Even at an airflow velocity of 4 m s^{-1} in the room air circulation case, which
327 corresponds to an air circulation rate of 80 h^{-1}, the magnitude of the air velocity inside the bin
328 was very low compared to the suction setup. The air velocity in the bin for the suction case
329 was higher than 1 m s^{-1} for all suction pressures. In the room air circulation case it was below
330 0.1 m s^{-1}. In the latter case, the airflow bypassed the bin and without any appreciable infiltration
331 in the porous region.

332 3.3.2 Deposition profile inside the bin

333 Fig. 9 depicts the droplet tracks and contours of droplet depositions for the tunnel and
334 room air circulation cases discussed in the previous section. For the suction case, droplets
335 deposited on fruit surfaces (targeted surface) and on non-targeted surfaces (bin and suction box
336 surfaces, floor and the plastic sheet that wraps the bin), dropped before reaching the stack, or
337 escaped the bin at the suction side. For the room air circulation case, droplets deposited on fruits

that are in the top region of the bin and mainly on other surfaces in the room (the walls, ceiling, door, floor, fruit bin, surfaces of the fans and evaporator unit). For the suction case, internal deposition was considerable (Fig. 9 (c)) while for the room air circulation case, there was almost no deposition inside the bin (Fig.9 (d)). Still, a considerable number of untreated fruits were found in both configurations (Fig. 9 (c) and (d).

Table 1 gives the amount deposited per square centimeter of fruit surface and a uniformity index of deposition. Increasing the suction pressure increased deposition on the fruit. For suction pressures above 50 Pa, more than 67% of the spray (1 L solution) was on-target. At a suction pressure of 500 Pa, deposition on fruit surfaces would amount to 80% of the total volume sprayed. On the other hand, depositions on fruit surfaces were very low for the room circulation cases and higher air circulation rates decreased deposition on fruit, leading to more off-target deposition. The maximum deposition was only 7.2 % of the volume sprayed at no air circulation. The uniformity index was calculated as the coefficient of variance (CV) of the local averaged droplet depositions at 27 sub-parts of the stack (dividing the fruit stack into 3×3×3 equal sized boxes).

The overall mean deposition on fruit surfaces was above 2 µL cm^{-2} in the suction configuration and the amount and uniformity increased (CV decreases with pressure, Table 1) with suction pressure. High suction increased the linear momentum of droplets that enhanced penetration into the stack internal region, improving uniformity of deposition: the CV dropped from 3.01 at 50 Pa to 1.93 at 500 Pa (Table 1).

The amount and uniformity of deposition from spraying on a single bin in the room was very poor. Droplets by-passed and missed the single stack in the room substantially. Loading the room fully with fruit would considerably reduce the by-pass flow and deposition higher than obtained here is expected. However, the magnitude of airflow through stacks in a fully loaded cool store room is still below 0.1 m s^{-1}(Ambaw et al., 2014), which is very low compared

to the level in the suction setup. Hence, the performance of spraying in a room is generally lower than spraying using the suction setup. Further analysis of factors affecting the spraying for the suction and room air circulation cases with CFD are discussed below.

3.4 Effect of droplet diameter and suction pressure on the distribution of droplet depositions

Finally, the effect of droplet diameter on deposition inside the bin was investigated. For this, the validated CFD model of the suction tunnel was used with sprays of similar sized spray droplets (15, 100, 200 and 300 μm) at 4 suction pressures (50, 167, 314 and 500 Pa). The air velocity, droplet velocity and cone angle of the spray nozzle in all models were the same. Fig. 10 (a) shows the fraction of the amount sprayed, depositing on fruit surfaces as a function of droplet diameter and suction pressure. Generally, deposition on fruit decreased with droplet size at a given suction pressure and increased with suction pressure at a given droplet size. At the highest suction pressure (500 Pa) the maximum amount of deposition was for the finest droplet size (15 μm) and the lowest deposition for the coarsest droplet size (300 μm).

Fig. 10 (b) shows the uniformity of deposition (expressed as coefficient of variance (CV) value) on fruit surfaces. The CV corresponding to the 15 μm droplets was above 3.0 whereas for the 200 and 300 μm droplets it was around 1.0, indicating, surprisingly, better uniformity characteristics of larger droplets. With suction pressure air velocity increases, resulting in an almost linear increase of deposition up to a critical value. For coarse droplets this value is higher (300 Pa) than for fine droplets (200 Pa). Apart from the finest and coarsest droplets (15 & 300 μm), the CV value also has a minimum close to the critical suction pressure. The results show that obtaining low CV values do not necessarily mean applying high suction pressure.

Fig. 11 compares the droplet trajectories and deposition profiles as a function of droplet diameter and suction pressure. The droplet trajectories originally followed the angle of discharge of the spray nozzle. Subsequently, it converged to the supporting air jet. This effect was stronger on fine droplets than on coarse droplets due to inertia. The flow path of spray of smaller droplets was consequently narrow in the first of the spray. As the air jet loses momentum it is deviated by the entrained airflow from the room approaching the bin. For fine droplets, thus a more concentrated spray plume hits the bin leading to relatively high CV values.

For coarse droplets with stronger inertia a more spread plume is first created, that however also converges again to some extent as well under the influence of entrained air, when the droplet velocity drops significantly. Still, it creates a more uniform spray hitting the bin, resulting in lower CV values of deposition.

Fig. 12 depicts contours of droplet deposition inside the stack. The color scale (<1 µL cm^{-2}) was set to maximize the visualization of the differentiation of depositions. As can be seen, deposition decreased with depth of the stack as a function of droplet size and suction pressures. Small droplets tended to deposit in the inlet region of the stack and did not reach the core of the stack. The enhanced lateral distribution of the 200 and 300 µm droplets in the stack is apparent in Fig. 12. Comparing, the 100 µm case with the 300 µm reveals that fine droplets deposited further in the stack, but entered the stack only on the center line with a reduced lateral dispersion. The 300 µm droplets entered the stack more uniformly but did not seem to deposit as deep as the 100 µm ones. 'Distributions of droplets in the axial and lateral directions are very important to sufficiently treat every fruit surface in the stack. However, depending on the size, different effects were observed. Coarse droplets performed best in terms of uniformity of deposition with more lateral dispersion, whereas fine droplets were entrained by the high velocity air and travel deep into the stack. In case of spraying stacked apple fruit, the penetration of droplets deep into the stack is an important characteristic. Hence, to retain the favourable

characteristics of fine droplets, implementation of multiple nozzles can be proposed to improve the lateral dispersion. This scenario was further investigated using the CFD model and proved effective (result not included).

Hoffmann et al. (2009) has concluded that sprayers producing larger droplets proved significantly better than the sprayers producing smaller droplets for deposition on vegetation in barrier applications. The reason for the poor performance of the smaller droplets in Hoffmann et al. (2009) was attributed to the ability of smaller droplets to float around and able to escape the measurement depth of 5 m in the canopy without deposition. Analysis of our result also showed that small droplets travelled deeper to the stack than larger droplets. For the case of stacked apple fruit this characteristics is very useful.

4 Conclusion and recommendations

This study assessed the spraying of a single bin filled with fruit and the subsequent deposition of droplets on fruit surfaces experimentally and by means of computational fluid dynamics (CFD). The CFD model successfully reproduced spraying in a tunnel and in a room.

Effects of suction pressure and droplet sizes on amount and uniformity of droplet deposition distribution were evaluated. None of the measured and simulated cases show an ideally uniform droplet deposition distribution. Spraying in a room in particular resulted in a very low amount of deposition. To this end, room spraying may not be advisable for application of plant control agents. Spraying in a tunnel configuration, which uses a dedicated suction system, on the other hand, looks a potential alternative. In this arrangement, individual bins can be treated in a spray tunnel before placing it in the cool store. Depending on the size, different effects were observed. Coarse droplets are best in terms of uniformity of deposition with more lateral dispersion whereas fine droplets have a very limited lateral dispersion and follow the high velocity air deep to the stack.

The circumstances inside a fully loaded cool store room are complex compared to the tunnel configuration or the single bin in a room presented in this study. The level of airflow is low and its path complex which requires dedicated experimental and numerical evaluation to improve performance. Further work will focus on developing and validation of more accurate models of spray atomization and surface interactions for this type of applications.

5 Acknowledgement

The Flemish Government (IWT contract 120745) and the Research Council of KU Leuven (postdoctoral grant for author A. Tsige), are gratefully acknowledged for financial support. This research was carried out in the context of the European COST Action FA1106 ("QualiFruit").

6 References

Ambaw, A., Verboven, P., Delele, M. A., Defraeye, T., Tijskens, E., Schenk, A., & Nicolai, B. M. (2014). CFD-based analysis of 1-MCP distribution in commercial cool store rooms: porous medium model application. Food and Bioprocess Technology, 7(7), 1903-1916.

Baker, K.F.. (1987). Evolving concepts of biological control of plant pathogens. Annual Review of Phytopathology, 25(1), 67-85.

Barth, M., Hankinson, T. R., Zhuang, H., & Breidt, F. (2009). Microbiological Spoilage of Fruits and Vegetables. Compendium of the microbiology spoilage of foods and beverages. In W. H. Sperber, & M. P. Doyle (Eds.), Food microbiology and food safety (pp. 135e183). Lake Forest: Springer Science þ Business Media, LLC.

Dahneke, B. (1971). The Capture of Aerosol Particles by Surfaces. J. ColloidInterf. Sci., 37:342–353.

Dekeyser, D., Vanwalleghem, T., Ambaw, A., Verboven, P., van Hemelrijck, W., Nuyttens, D.. (2015).Technical performance of fogging applications of biological control organisms in fruit cold storage rooms. Julius-Kühn-Archiv, 448, p. 68.

Delele, M. A., Jaeken, P., Debaer, C., Baetens, K., Endalew, A. M., Ramon, H., ... & Verboven, P. (2007). CFD prototyping of an air-assisted orchard sprayer aimed at drift reduction. *Computers and Electronics in Agriculture*, *55*(1), 16-27.

Delele, M., Vorstermans, B., Creemers, P., Tsige, A. A., Tijskens, E., Schenk, A., Opara, U. L., Nicolaī, B., & Verboven, P. (2012a). CFD model development and validation of a thermonebulisation fungicide fogging system for postharvest storage of fruit. Journal of Food Engineering, 108(1), 59–68.

Delele, M. A., Vorstermans, B., Creemers, P., Tsige, A. A., Tijskens, E., Schenk, A., Opara, U. L., Nicolaï, B. M., & Verboven, P. (2012b). Investigating the performance of thermonebulisation fungicide fogging system for loaded fruit storage room using CFD model. Journal of Food Engineering, 109, 87–97.

Delele, M.A., Nuyttens, D., Duga, A.T., Ambaw, A., Lebeau, F., Nicolai, B., and Verboven, P. (2016). Predicting the dynamic impact behaviour of spray droplets on flat 1 plant surfaces. Soft Matter, 2016, DOI: 10.1039/C6SM00933F.

Droby, S., Lechter, A. (2004). Postharvest botrytis infection: etiology, development and management. In: Elad, Y., Williamson, B., Tudzynski, P., Delen, N. (Eds.), Botrytis: Biology, Pathology and Control. Kluwer Academic Publishers, 428, 349–367.

Droby, S., Wisniewski, M., El Ghaouth, A. and Wilson, C.L. (2003). Biological control of postharvest diseases of fruits and vegetables: current advances and future challenges. Acta Horticulturae 628, 703–713.

Duga, A. T., Dekeyser, D., Ruysen, K., Bylemans, D., Nuyttens, D., Nicolai, B., & Verboven, P. (2015). Challenges for CFD modeling of drift from air assisted orchard sprayers. Julius-Kühn-Archiv, (448), 34.

Endalew, A. M., Debaer, C., Rutten, N., Vercammen, J., Delele, M. A., Ramon, H., ... & Verboven, P. (2010). A new integrated CFD modelling approach towards air-assisted

485 orchard spraying. Part I. Model development and effect of wind speed and direction on
486 sprayer airflow. Computers and electronics in agriculture, 71(2), 128-136.

487 Foque, D., Dekeyser, D., Zwertvaegher, I., Nuyttens, D. (2014). Accuracy of a multiple mineral
488 tracer methodology for measuring spray deposition. Asp. Appl. Biol. 122, 203-212.

489 Francesco A. Di., Mari, M.. (2014). Use of biocontrol agents in combination with physical and
490 chemical treatments: efficacy assessments Stewart Postharvest Rev., 1–2, 1–4.

491 Franke J, Hellsten A, Schlünzen H, Carissimo B (2007) Best practice guideline for the CFD
492 simulation of flows in the urban environment. COST Action 732: Quality assurance and
493 improvement of microscale meteorological models, Hamburg, Germany.

494 Gustavsson, J., Cederberg, C., Sonesson, U., van Otterkijk, R., Meybeck, A. (2011). "Global
495 Food Losses and Food Waste: Extent, Causes, and Prevention." Food and Agriculture
496 Organization of the United Nations, Rome.

497 Hoffmann, W.C., Farooq, M., Walker, T.W., Fritz, B., Szumlas, D., Quinn, B., Bernier, U.,
498 Hogsette, J., Lan, Y., Huang, T., Smith, V.L., Robinson, C.A. (2009). Canopy penetration
499 and deposition of barrier sprays from electrostatic and conventional sprayers. J Am Mosq
500 Control Assoc 25:323–331.

501 Jain, S., & Petrucci, G. A. (2015). A New Method to Measure Aerosol Particle Bounce Using
502 a Cascade Electrical Low Pressure Impactor. Aerosol Science and Technology, 49(6), 390-
503 399.

504 Janisiewicz, W.J., Korsten, L., 2002. Biological control of postharvest diseases of fruit. Annual
505 Review of Phytopathology 40, 411–441.

506 Mahajan, P.V., Caleb, O.J., Singh, Z., Watkins, C.B., Geyer, M. (2014). Postharvest treatments
507 of fresh produce. Phil. Trans. R. Soc. A 372, 20130309.

508 Nuyttens D, Baetens K, De Schampheleire M, Sonck B. 2007a. Effect of Nozzle Type, Size
509 and Pressure on Spray Droplet Characteristics. Biosystems Engineering. 97 (3) 333–345.

510 Nuyttens D, De Schampheleire M, Baetens K, Sonck B. 2007b. The influence of operator
511 controlled variables on spray drift from field crop sprayers. Transactions of the ASABE
512 50(4): 1129–1140.

513 Roache PJ, (1994) Perspective: a method for uniform reporting of grid refinement studies.
514 Transactions of the ASME - Journal of Fluids Engineering 116 (3), 405-413.

515 Wisniewski, M., Wilson, C., El Ghaouth, A., Droby, S., 2001. Non-chemical approaches to
516 postharvest disease control. Acta Hort. 553, 407–412.

517 Wisniewski, M., Wilson, C., Droby, S., Chalutz, E., El Ghaouth, A., Stevens, C., 2007.
518 Postharvest biocontrol: new concepts and applications. In: Vincent, C., Goettel, M.S.,
519 Lazarovits, G. (Eds.), Biological Control A Global Perspective. CABI, Cambridge, MA,
520 USA, pp. 262–273.

521

522 Table 1. Simulated droplet deposition distributions for the droplet size spectra of the Fontan®
523 Starlet ULV 92 cold fogger at a spraying rate of 5.2 L h^{-1}. In each case 1 L of water was
524 sprayed within 12 min. CV is the coefficient of variance calculated from the area-averaged
525 deposition values of 3 × 3 × 3 block regions inside the bin.

	Case	Deposition (µL cm^{-2})	CV surfaces (−)	Total on fruit (L)	Total on non-target surfaces (L)	Escaped (L)
Suction	50 Pa	2.18	3.01	0.67	0.24	0.09
	167 Pa	2.44	2.55	0.75	0.18	0.07
	314 Pa	2.73	2.04	0.84	0.12	0.04
	500 Pa	2.82	1.93	0.84	0.11	0.05
Room	0 m/s	0.23	4.7	0.07	0.93	–
circulation	2 m/s	0.13	6.34	0.04	0.96	–
	4 m/s	0.06	9.89	0.02	0.98	–

526

527

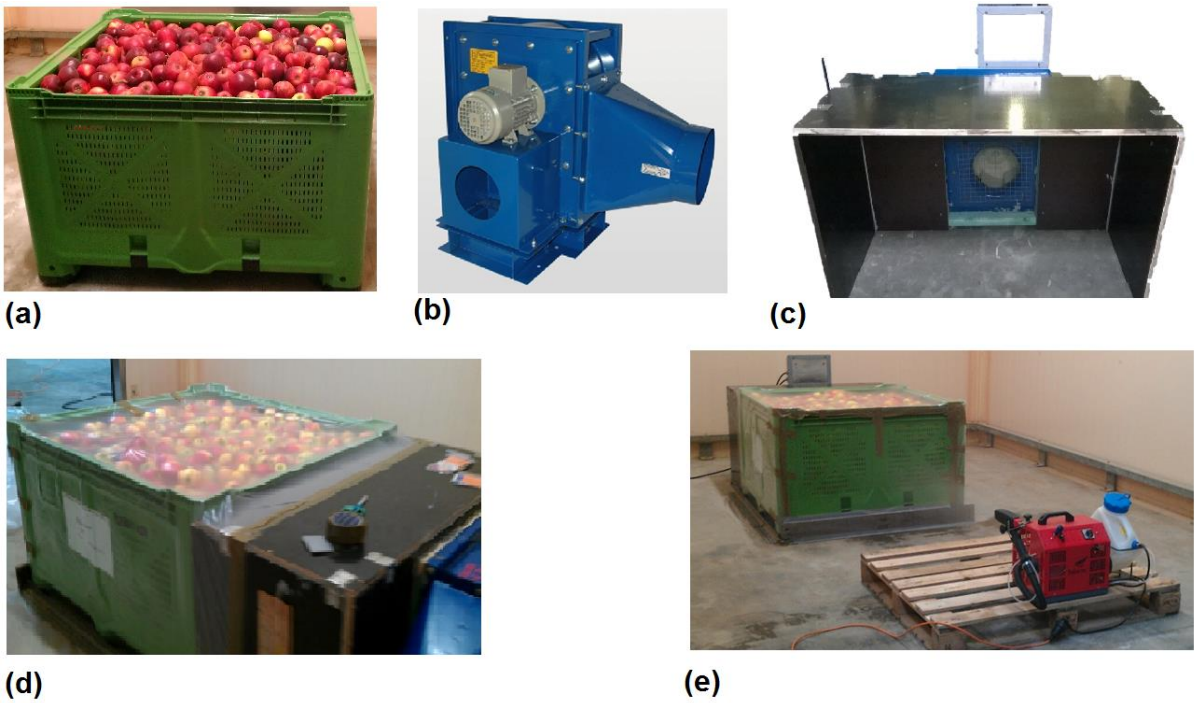

Fig. 1. Experimental setup for the spray application on a single bin. (a) Fruit loaded plastic bin (the stack), (b) centrifugal fan, (c) box and fan assembly forming the suction tunnel, (d) the stack as wrapped with a thin plastic sheet and connected air tight to the suction tunnel and (e) the full experimental setup showing the spray application in a tunnel. The whole assembly was placed inside a cool room at ambient condition ≈10°C and RH of 90%. During the spraying the door of the cool room was closed and the air circulation fan of the evaporator in the cool room was turned off. Spraying was by Fontan® Starlet ULV 92 cold fogger. See the schematic in Fig. 4.

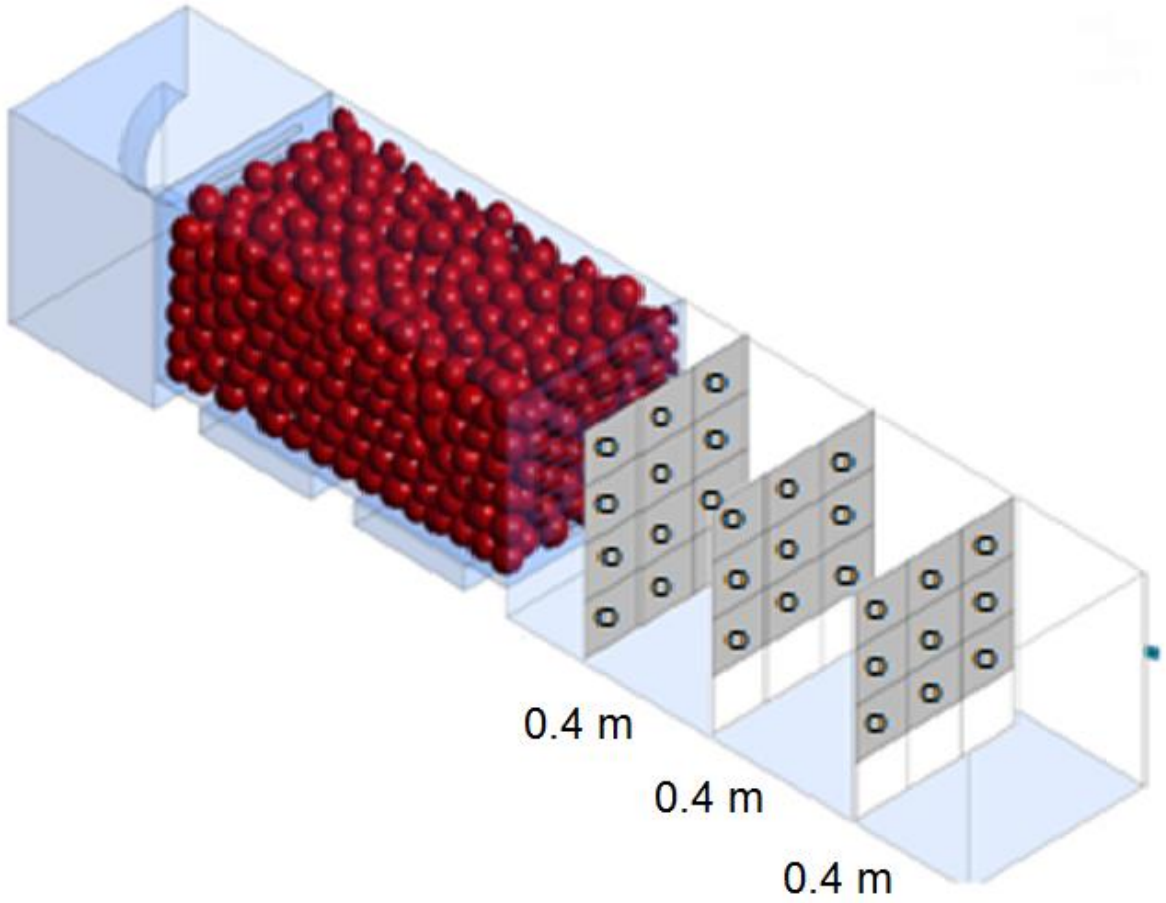

Fig. 2. Schematic of symmetric half of the experimental setup showing the position of the velocity sampling grids with the measuring points circled. The distance between two measuring points on a plane was 0.15 m. During velocity measurement, the spray nozzle was running dry (without spraying).

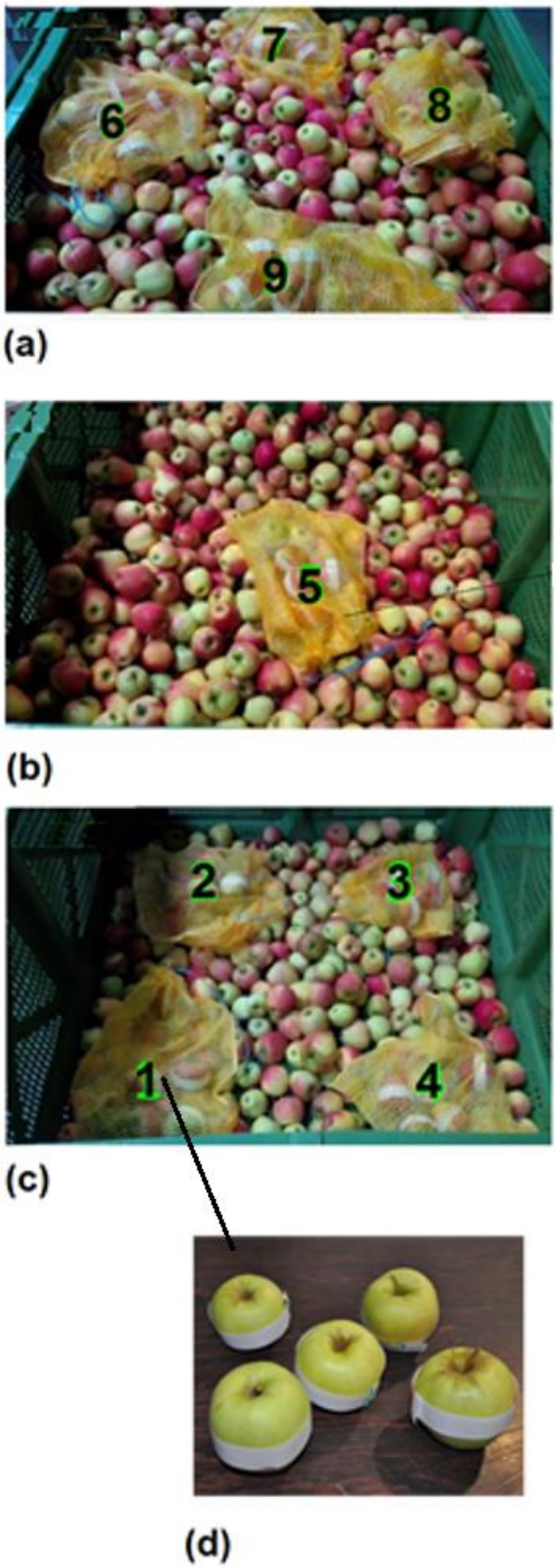

Fig. 3. Sampling positions for analysis of tracer deposits. (a) top region of the stack, (b) middle region of the sack, (c) bottom region of the stack and (d) filter paper wrapped around the equator of the apple fruits to sample the tracer depositions. At each sampling position five filter paper wrapped apple fruits were enclosed in a foldable plastic bag.

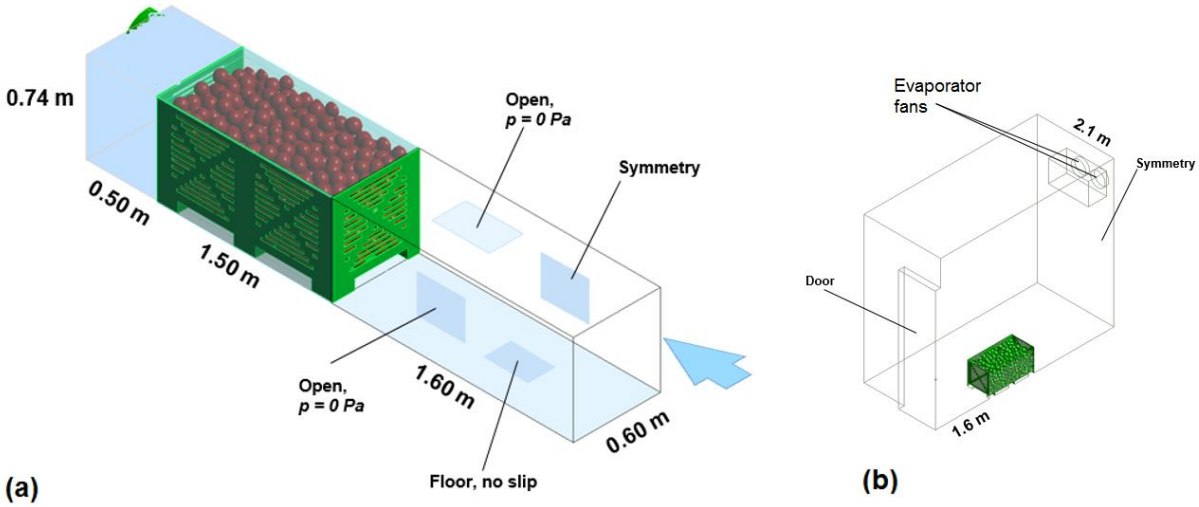

Fig. 4.Geometry and boundary conditions of the CFD models of the tunnel experiment (a) and spraying on a single stack in a cool room (b).

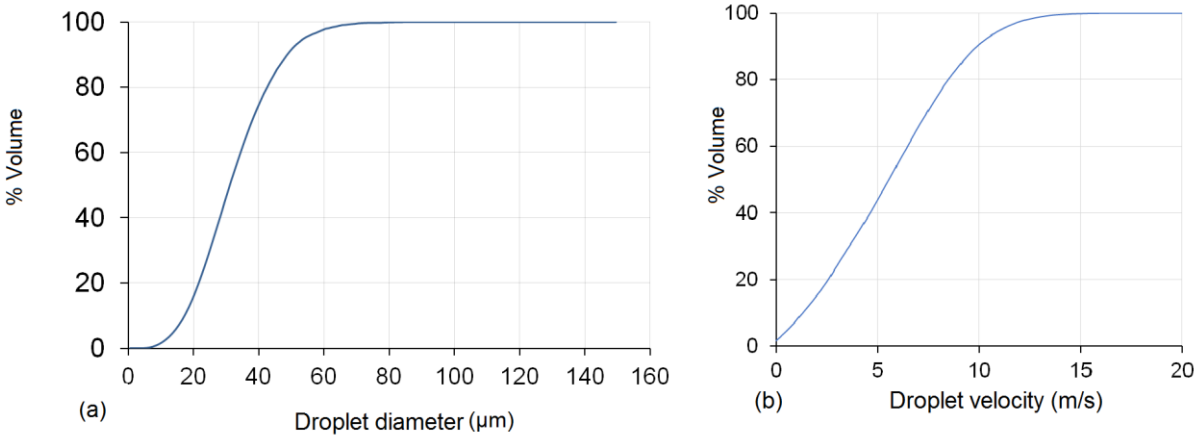

Fig. 5. Droplet diameter (a) and droplet velocity (b) distributions of the Fontan® Starlet ULV 92 cold fogger as measured using a PDPA laser at distances of 0.50 m from the outlet opening. The spray device has a spraying rate of 5.2 L h^{-1}.

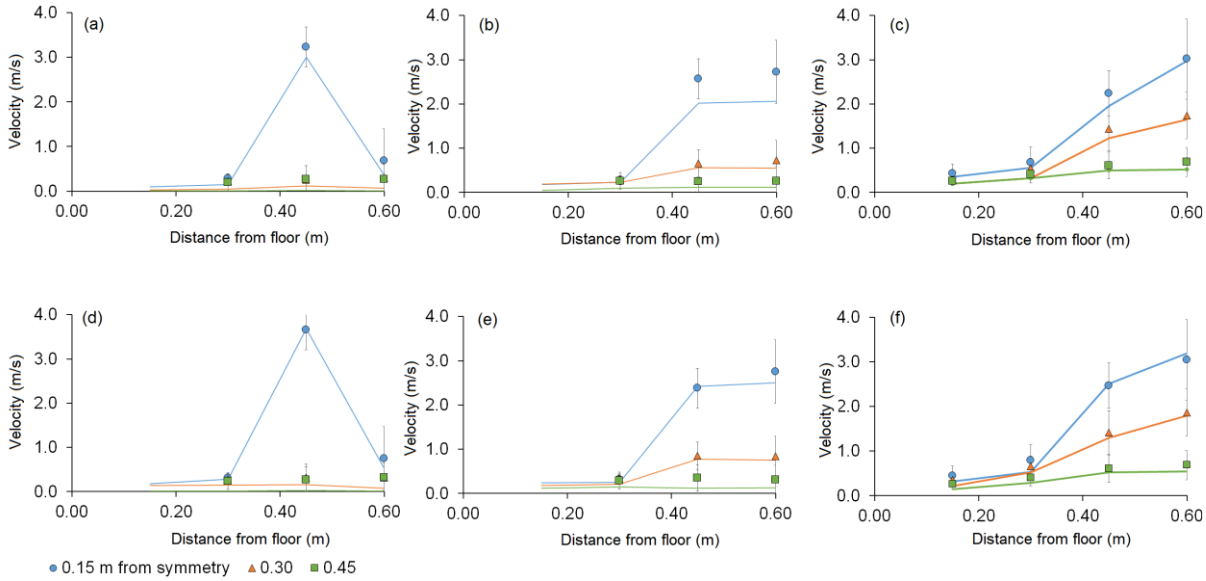

Fig. 6. Measured and simulated total air velocity values in front of the fruit stack in a tunnel

under suction pressure of 167 Pa (top row) and 314 Pa (bottom row). Measurement were taken at grid points on vertical planes at 0.4m from the nozzle ((a) and (d)), 0.8m from the nozzle ((b) and (e)) and 1.2m from the nozzle ((c) and (f)). The velocity measurement grids are shown in Fig. 3. Curves correspond to simulated values and symbols to experimental measurements. Measurements were done 3 times. Vertical bars indicate standard deviations.

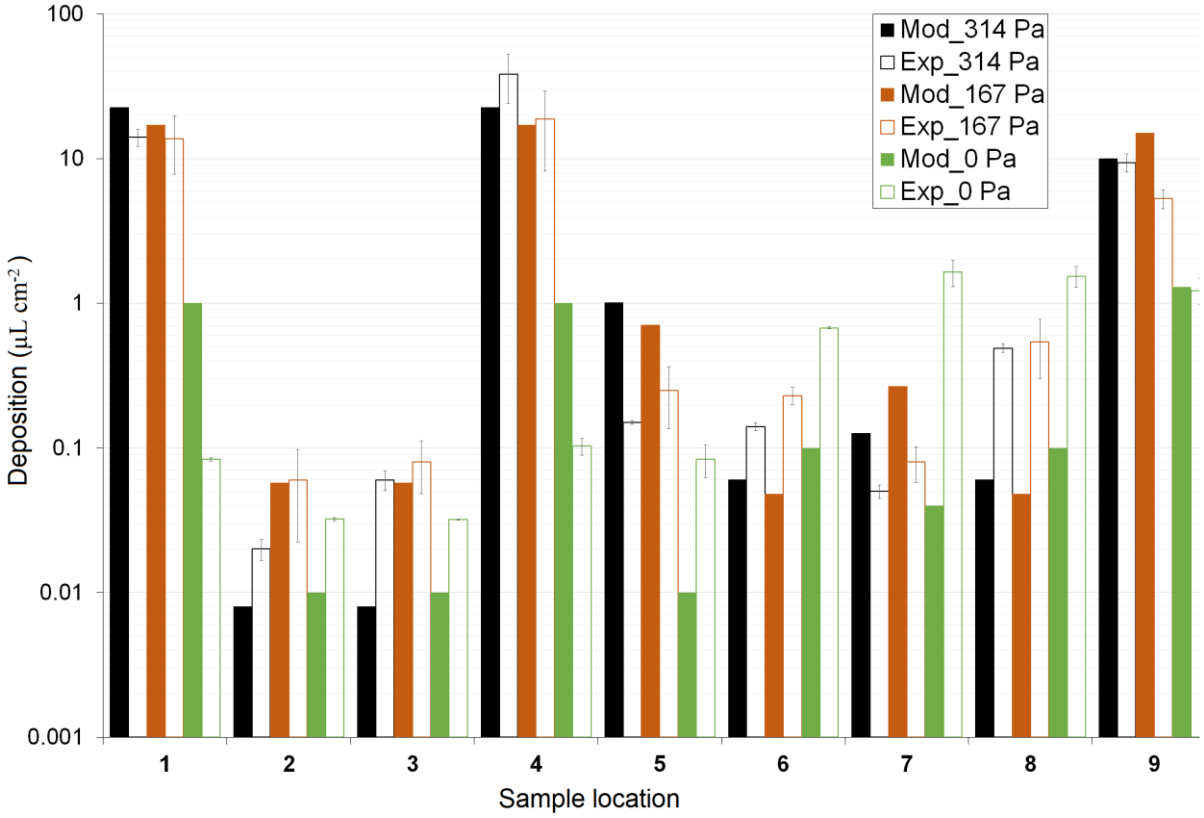

Fig. 7. Measured (filled squares) and simulated (empty squares) mean droplet depositions per sample position (see Fig. 3) from spraying a bin in a tunnel and in a room. Filter papers were wrapped around the equator of 5 apple fruits to collect depositions per position. In each case 1L of tracer solution was sprayed using the Fontan® Starlet ULV 92 cold fogger within 12 ± 1 min. Measurement were done 2 times. Vertical bars indicate standard deviations.

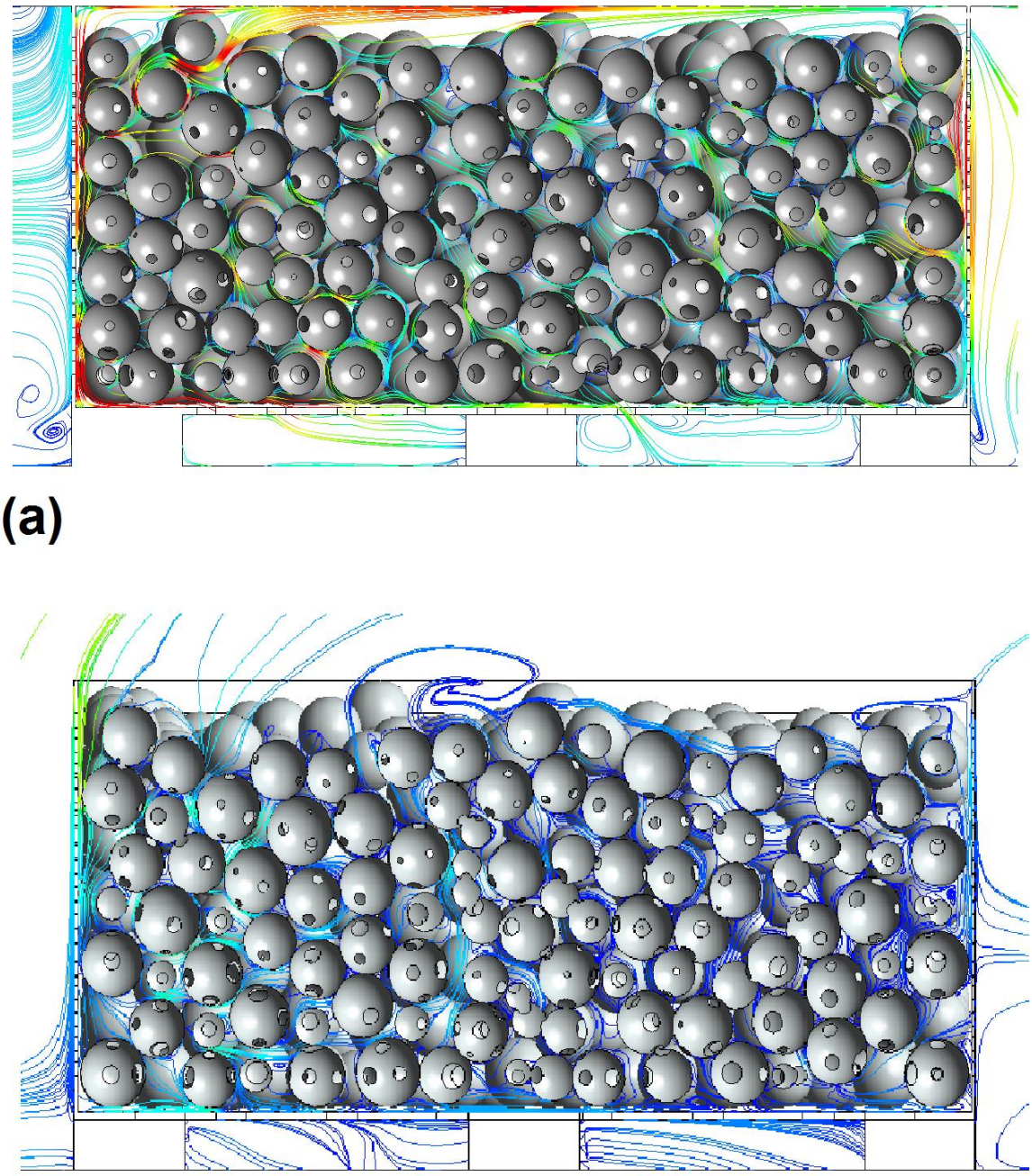

Fig. 8. Simulated air velocity streamlines on symmetry plane in the bin in the tunnel at a suction pressure of 50 Pa (a) and in the bin in the room at a fan air velocity of 4 m s^{-1} (Room air exchange rate of 80 h^{-1}) (b).

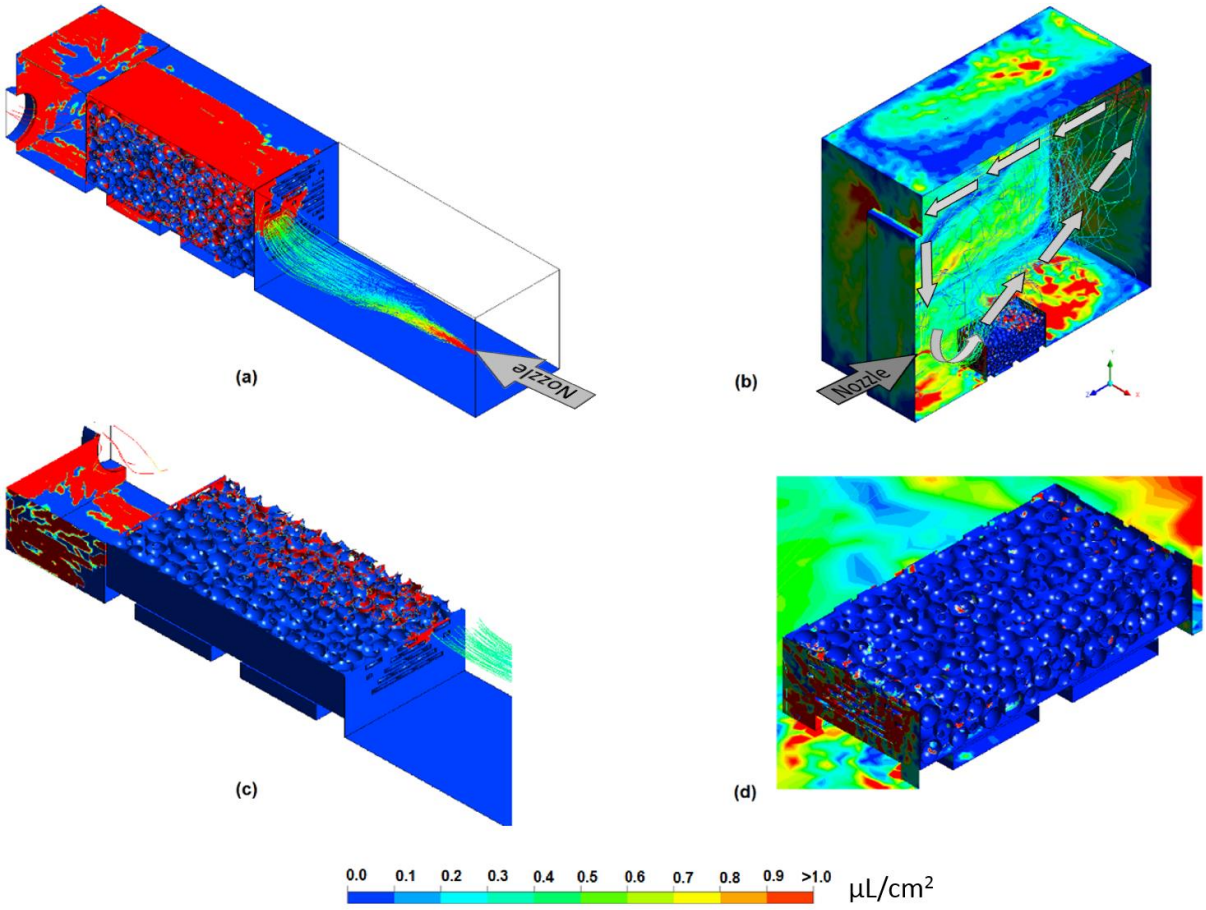

572
573 Fig. 9. Simulated profile of particle track and contour of droplet depositions in a tunnel at
574 suction pressure of 50 Pa (a) and in room at fan airflow velocity of 4 m s^{-1} (b). Penetration of
575 spray droplets are shown by removing the top half of the pallet in the tunnel (c) and in the room
576 (d). Arrows indicate the overall direction of airflow and particle trajectory. The colour on the
577 particle tracks (red (4 m/s), blue (0 m/s)) indicates droplet velocity.

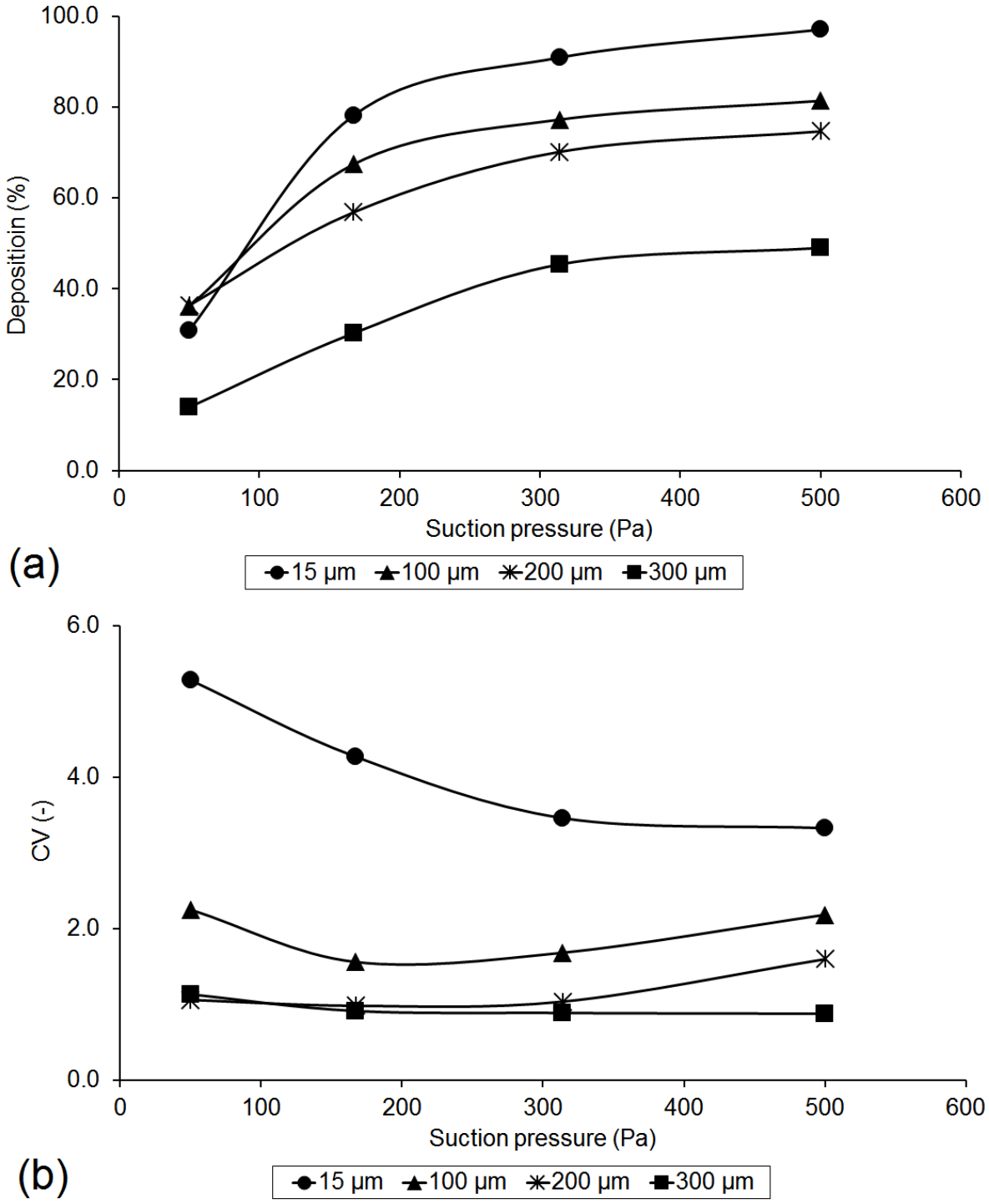

578
579 Fig. 10. Effect of droplet size on the relative amount deposited (a) and uniformity of deposits
580 (expressed as CV value) on fruit surfaces (b). In each case 1L of tracer solution was sprayed
581 within 12 ± 1 min. The coefficient of variance (CV) of depositions was calculated from values
582 obtained at sampling positions inside the stack as shown in Fig. 3.

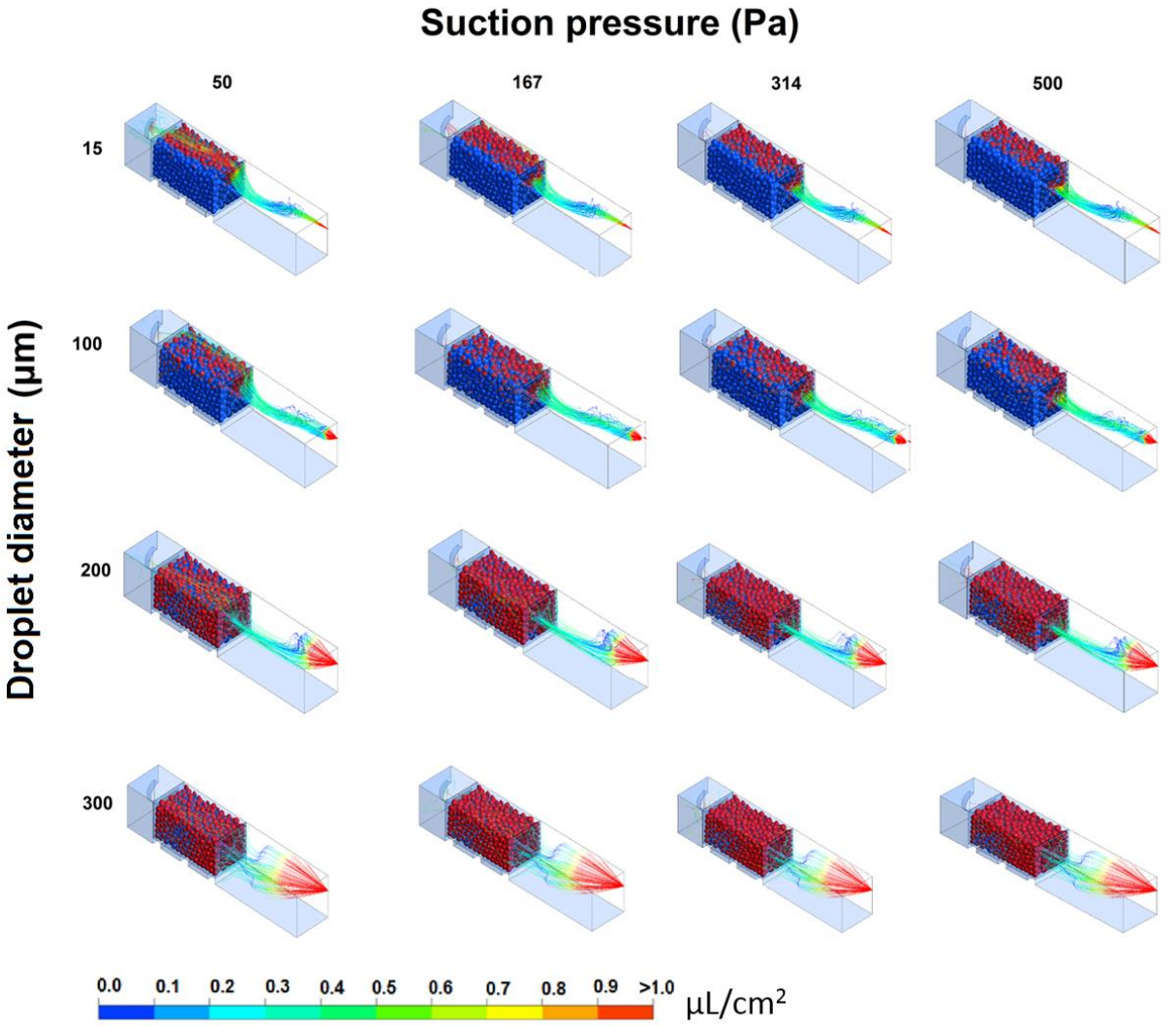

Fig. 11. Simulated droplet particle tracks and depositions on as a function of droplet diameter and suction pressures. Each simulation corresponds to spraying 1L of water within 12 ± 1 min. The colour on the particle tracks (red (4 m/s), blue (0 m/s)) indicates droplet velocity.

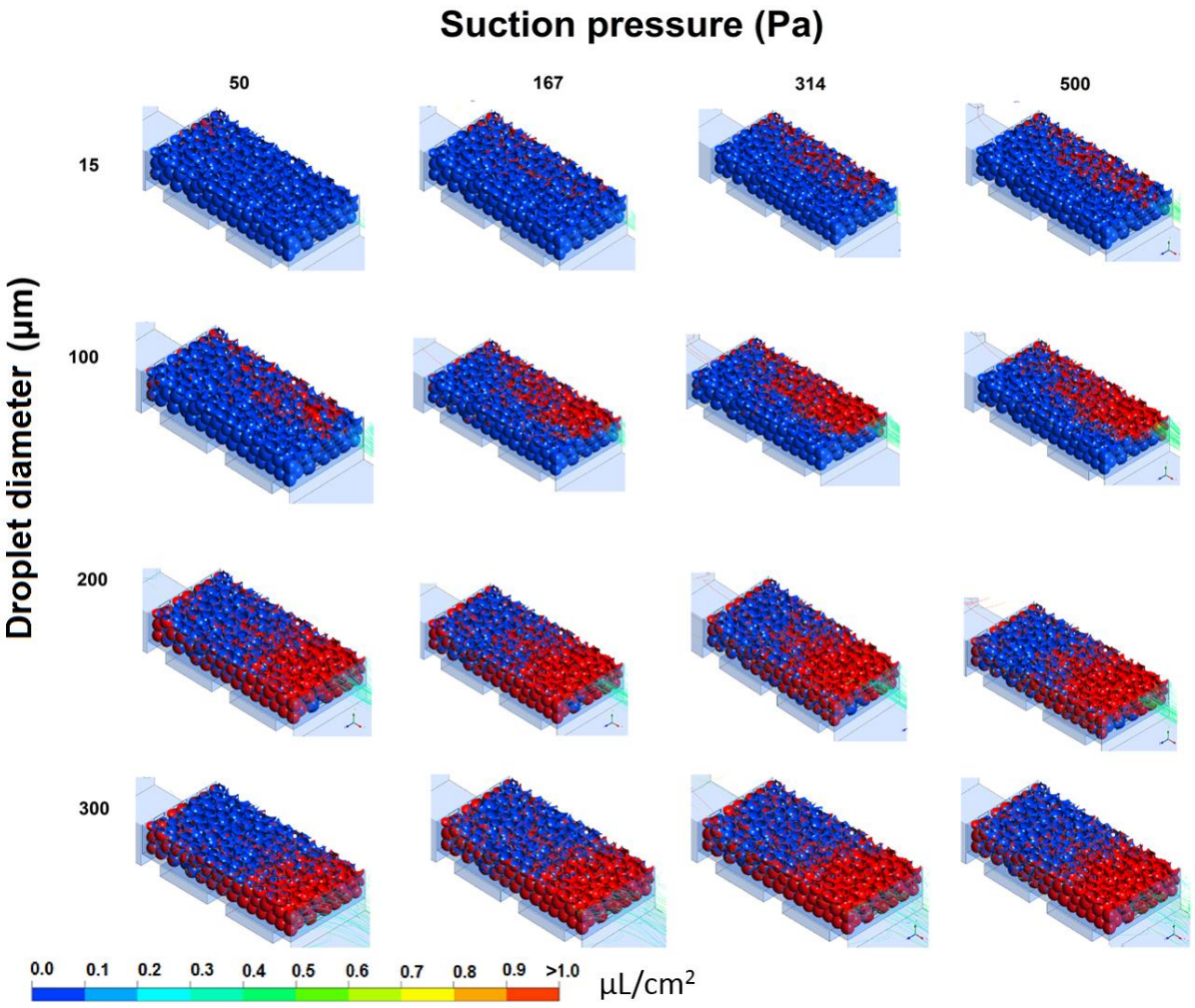

Fig. 12. Simulated droplet depositions in the stack internal surfaces as a function of droplet size and suction pressures. Each simulation corresponds to spraying 1L of water within 12 ± 1 min.